CHAPTER VI

Experiments

6.1 Calibration and Reconstruction Error

This experiment was set up for accuracy testing of developed system when one or two of 4-cameras cannot detect the object. Chessboard No.1 was used to provide 3-D world points in both calibration and reconstruction process. Table 6.1 shows the reference number of camera with their corresponding serial number. Tsai's calibration method and Zhang's calibration method were used to calibrate four cameras and the results of calibration are shown in table 6.2-6.5, where R_x, R_y and R_z is x, y and z components of Rodrigues's formula.

Table 6.1: Camera number with corresponding serial number.

Camera No.	1	2	3	4
Serial Number	7410265	7411015	7411064	7411065

Table 6.2: Camera No.1 calibration result.

Parameter	Tsai's calibration	Zhang's calibration
α_x	2601.6963	2642.8012
α_y	2601.6963	2631.8707
s	0.0000	-15.6053
u_0	640.0000	565.6320
v_0	512.0000	509.9550
k_1	0.1155	-0.0198
k_2	0.0000	1.1116
R_x	1.1360	1.0899
R_y	2.5652	2.6106
R_z	-0.6860	-0.7040
t_x	-0.0441	0.0153
t_y	0.0768	-0.0905
t_z	1.0142	1.0405

Table 6.3: Camera No.2 calibration result.

Parameter	Tsai's calibration	Zhang's calibration
α_x	2569.8052	2550.2196
α_y	2569.8052	2537.9607
s	0.0000	-38.5084
u_0	640.0000	534.3520
v_0	512.0000	529.0935
k_1	0.05202	-0.0045
k_2	0.0000	0.1633
R_x	2.3897	2.3767
R_y	1.1092	1.1849
R_z	-0.2627	-0.2867
t_x	-0.1032	-0.0459
t_y	-0.0270	-0.0366
t_z	0.9624	0.9577

Table 6.4: Camera No.3 calibration result.

Parameter	Tsai's calibration	Zhang's calibration
α_x	2347.5274	2509.1108
α_y	2347.5274	2473.5991
s	0.0000	-32.6602
u_0	640.0000	621.4908
v_0	512.0000	470.1164
k_1	0.0102	-0.0015
k_2	0.0000	0.1964
R_x	2.5039	2.5135
R_y	-0.9567	-0.9667
R_z	0.2337	0.2570
t_x	-0.0003	0.0102
t_y	0.0507	0.0719
t_z	0.8216	0.8781

Table 6.5: Camera No.4 calibration result.

Parameter	Tsai's calibration	Zhang's calibration
α_x	2546.1458	2450.9561
α_y	2546.1458	2464.1788
s	0.0000	8.4558
u_0	640.0000	593.8771
v_0	512.0000	552.4781
k_1	-0.2852	-0.0151
k_2	0.0000	0.9102
R_x	1.1730	1.1741
R_y	-2.6700	-2.6546
R_z	0.6631	0.6351
t_x	0.0957	0.1179
t_y	0.0026	-0.0149
t_z	0.9042	0.8696

The error of calibration in each camera is defined by geometric distance which is a summation of square of the difference between measured and estimated image coordinates. Table 6.6 shows the geometric distance of each calibrated camera.

Table 6.6: Geometric distance

Camera No.	Tsai's Method ($pixel^2$)	Zhang's Method ($pixel^2$)
1	9.7566	7.5982
2	7.7782	9.6145
3	11.9442	12.0656
4	17.3126	8.1062

For reconstruction error, four cameras had been used to capture image of chessboard calibration pattern and linear triangulation with Least-Squares had been used as reconstruction method. The reconstruction error which is distance between reconstruction point and 3-D world points which are provided by chessboard pattern are shown in table 6.7.

Table 6.7: 3-D reconstruction error from linear triangulation method

Camera No.				Tsai's Method (mm)			Zhang's Method (mm)		
1	2	3	4	mean	sd	max	mean	sd	max
✓	✓	✓	✓	0.0826	0.0364	0.1495	0.0778	0.0360	0.2224
	✓	✓	✓	0.0972	0.0449	0.1750	0.0777	0.0330	0.1949
✓		✓	✓	0.1075	0.0478	0.2182	0.0903	0.0409	0.2654
✓	✓		✓	0.0988	0.0420	0.1952	0.0720	0.0343	0.1397
✓	✓	✓		0.0886	0.0482	0.2140	0.0881	0.0442	0.2951
✓	✓			0.1106	0.0667	0.2435	0.0985	0.0454	0.2038
✓		✓		0.1107	0.0571	0.2544	0.1020	0.0558	0.3569
✓			✓	0.1745	0.1025	0.4611	0.0679	0.0319	0.1296
	✓	✓		0.1034	0.0611	0.2832	0.1016	0.0422	0.2474
	✓		✓	0.1201	0.0461	0.2068	0.0766	0.0341	0.1560
		✓	✓	0.2138	0.1079	0.4415	0.1104	0.0592	0.3189

This experiment shows that both Tsai' calibration method and Zhang's calibration method can be used in camera calibration process with the same accuracy. The geometric distance, which obtained from Tsai's calibration method, is very close to the geometric distance obtained from Zhang's calibration method. For 3 and 4 cameras system, the maximum reconstruction error when use camera models, which obtained from Tsai' calibration method, is usually less than Zhang's calibration method.

6.2 3-D Tracking for Direct Linear Motion with S-Curve Profile

The experiment was set up for motion tracking of moving object which moved with direct linear motion with s-curve velocity profile. PA10-7C arm had been used to generate motion of the target in x, y and z direction in robot frame. 3-D path with 300 mm in displacement was generated in each direction. For the best accuracy, circle with center mark had been used as target instead of spherical ball. The camera parameters of the camera models used in this experiment are shown in table 6.8.

Table 6.8: Camera parameters of camera models used in motion tracking experiments.

Parameter	Camera No.1	Camera No.2	Camera No.3	Camera No.4
α_x	2620.2143	2425.5940	2350.2705	2455.4462
α_y	2620.2143	2425.5940	2350.2705	2455.4462
s	0.0000	0.0000	0.0000	0.0000
u_0	640.0000	640.0000	640.0000	640.0000
v_0	480.0000	480.0000	480.0000	480.0000
k_1	0.2690	0.1926	0.2517	0.4000
k_2	0.0000	0.0000	0.0000	0.0000
R_x	-2.9337	-2.9784	-2.9787	-2.9541
R_y	-0.0421	-0.0115	-0.0219	0.0482
R_z	0.4848	0.1525	-0.2093	-0.5155
t_x	-0.0681	-0.0685	-0.0839	-0.0640
t_y	0.1428	0.1442	0.1650	0.1442
t_z	2.9390	2.9235	2.8480	2.6391

In order to map the detected coordinate from the developed vision system's reference frame to PA10-7C arm's frame, the maximum likelihood with Levenberg-Marquardt optimization has been used. The transformation matrix obtained with this algorithm is:

$$\mathbf{T} = \begin{bmatrix} -0.0393 & -0.0901 & 0.9952 & 4.4795\times10^{-3} \\ 0.9991 & -0.0208 & 0.0375 & -66.8072\times10^{-3} \\ 0.0174 & 0.9957 & 0.0909 & 716.6457\times10^{-3} \\ 0.0000 & 0.0000 & 0.0000 & 1.0000 \end{bmatrix}$$

The system was set up as show in figure 6.1 where subscript r is referred to PA10-7C robotic arm reference frame.

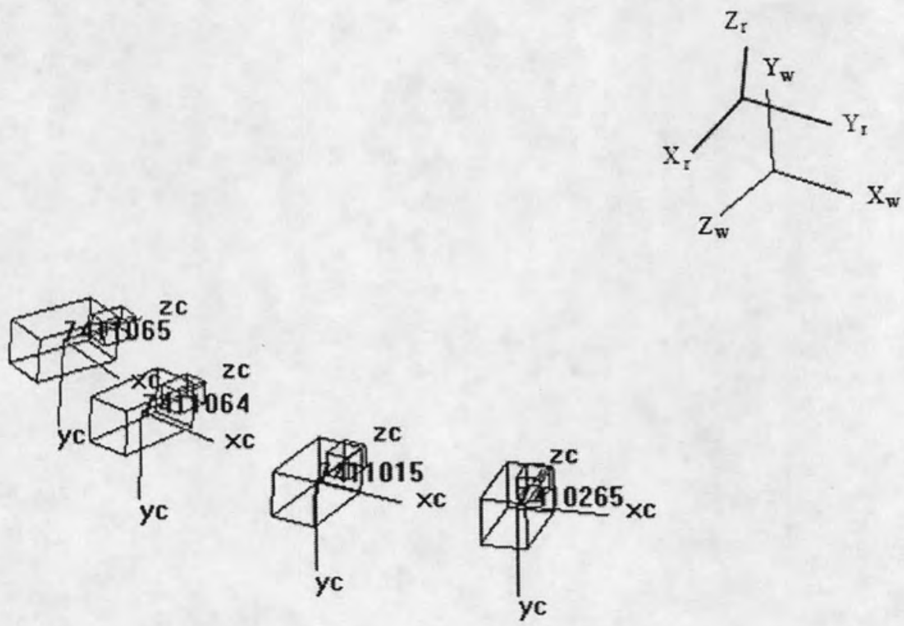

Figure 6.1: System set up for 3-D tracking experiments.

6.2.1 Using 4-Cameras

The following experiment used 4 cameras to track motion of target. The tracking results are shown in figure 6.2–6.10.

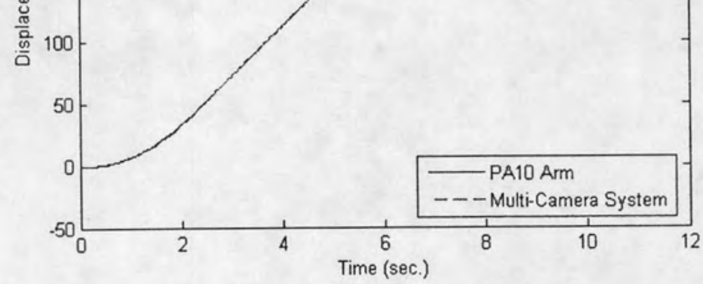

Figure 6.2: Linear motion in x direction of PA10 arm with acceleration and deceleration 20 mm/s^2, velocity 40 mm/s and displacement 300 mm. (4-Cameras)

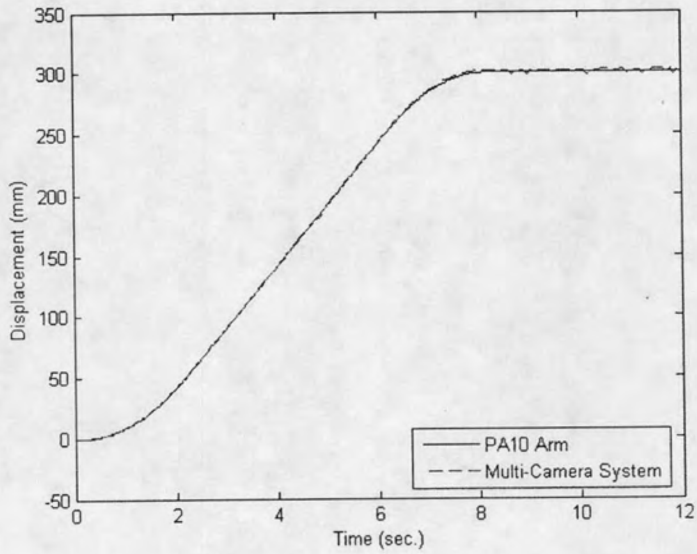

Figure 6.3: Linear motion in x direction of PA10 arm with acceleration and deceleration 25 mm/s^2, velocity 50 mm/s and displacement 300 mm. (4-Cameras)

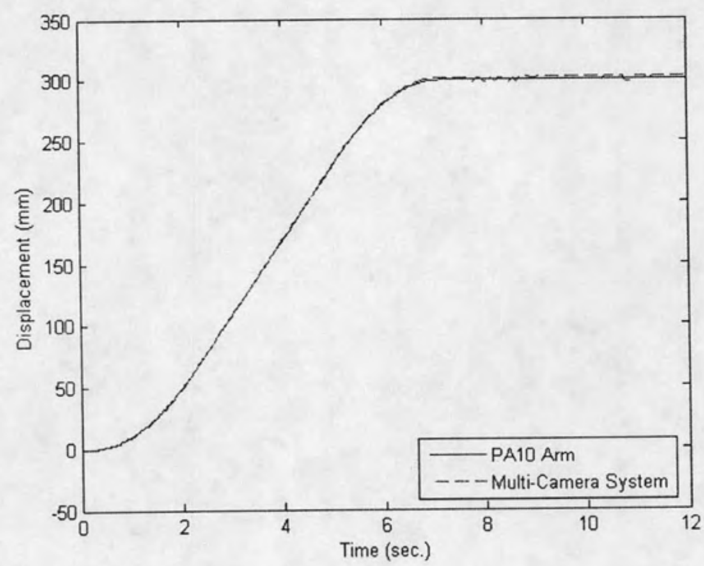

Figure 6.4: Linear motion in x direction of PA10 arm with acceleration and deceleration 30 mm/s^2, velocity 60 mm/s and displacement 300 mm. (4-Cameras)

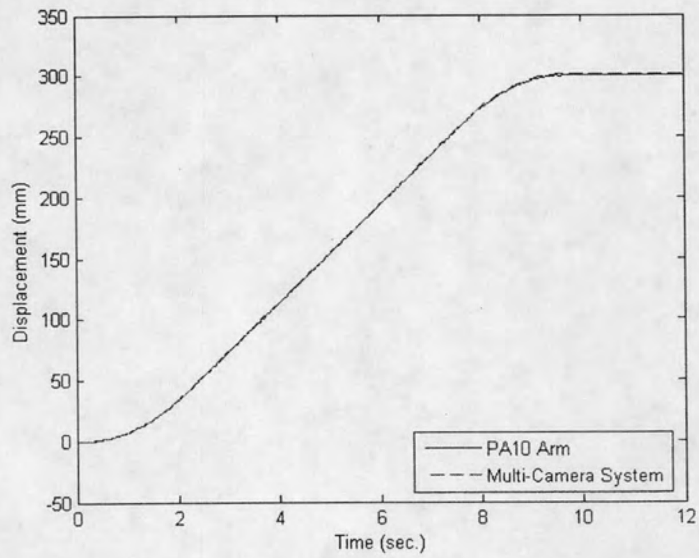

Figure 6.5: Linear motion in y direction of PA10 arm with acceleration and deceleration $20\ mm/s^2$, velocity 40 mm/s and displacement 300 mm. (4-Cameras)

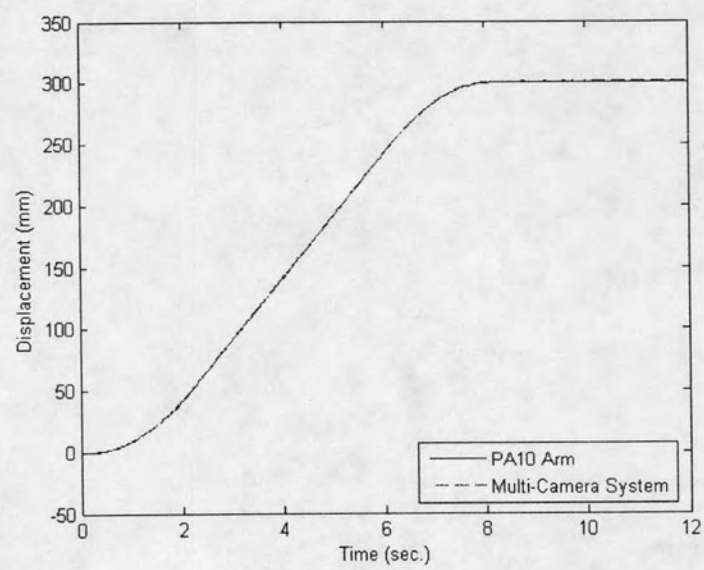

Figure 6.6: Linear motion in y direction of PA10 arm with acceleration and deceleration $25\ mm/s^2$, velocity 50 mm/s and displacement 300 mm. (4-Cameras)

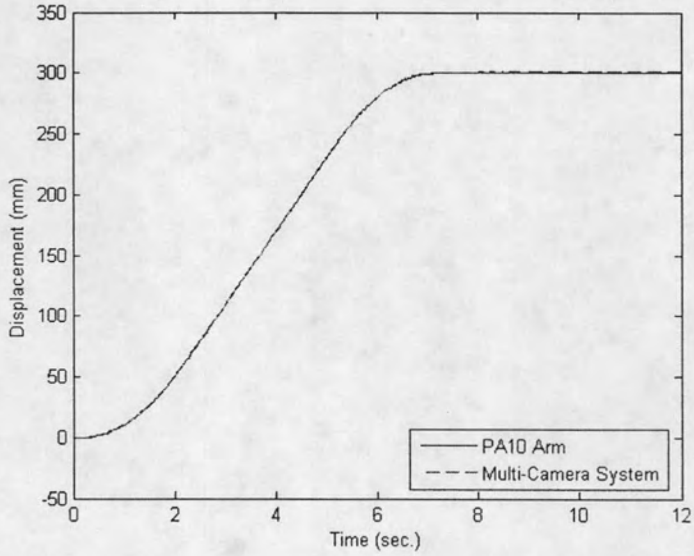

Figure 6.7: Linear motion in y direction of PA10 arm with acceleration and deceleration 30 mm/s^2, velocity 60 mm/s and displacement 300 mm. (4-Cameras)

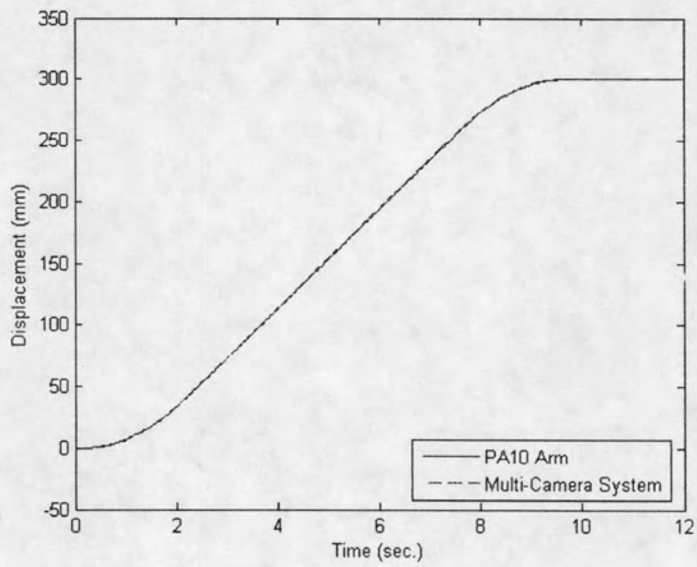

Figure 6.8: Linear motion in z direction of PA10 arm with acceleration and deceleration 20 mm/s^2, velocity 40 mm/s and displacement 300 mm. (4-Cameras)

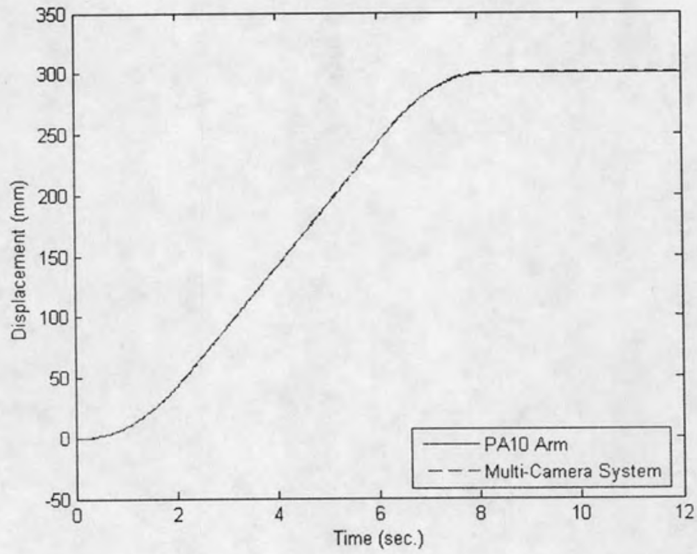

Figure 6.9: Linear motion in z direction of PA10 arm with acceleration and deceleration 25 mm/s^2, velocity 50 mm/s and displacement 300 mm. (4-Cameras)

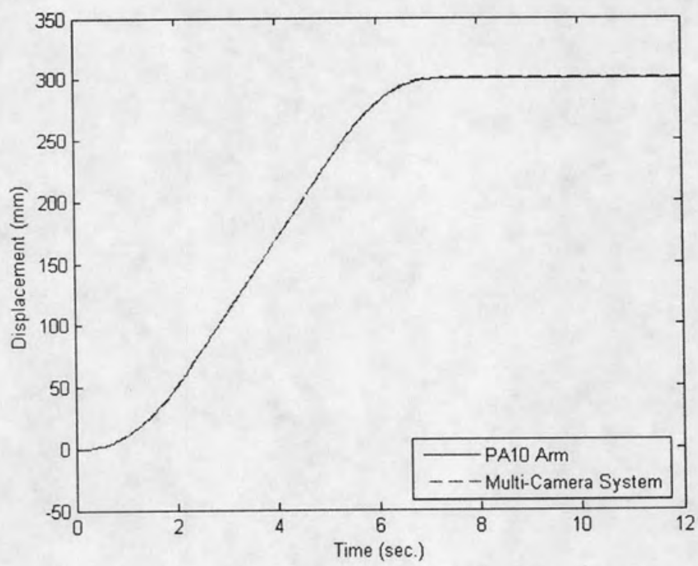

Figure 6.10: Linear motion in z direction of PA10 arm with acceleration and deceleration 30 mm/s^2, velocity 60 mm/s and displacement 300 mm. (4-Cameras)

6.2.2 Using 3-Cameras

The following experiment used 3 cameras. The tracking results are shown in figure 6.11–6.19.

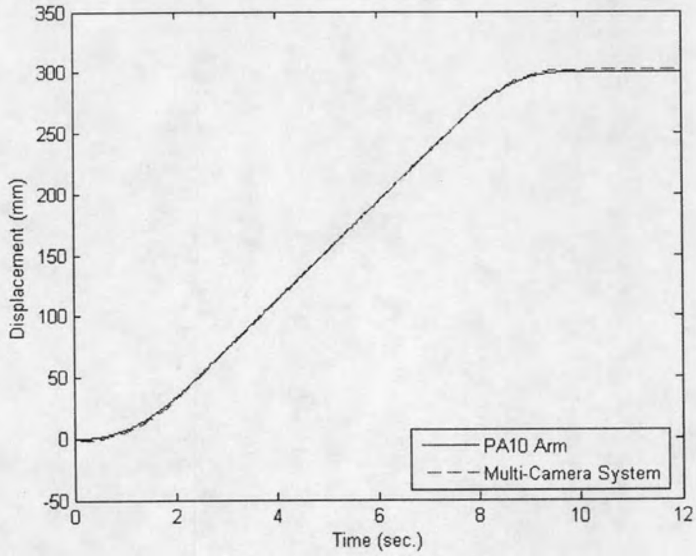

Figure 6.11: Linear motion in x direction of PA10 arm with acceleration and deceleration 20 mm/s^2, velocity 40 mm/s and displacement 300 mm. (3-Cameras)

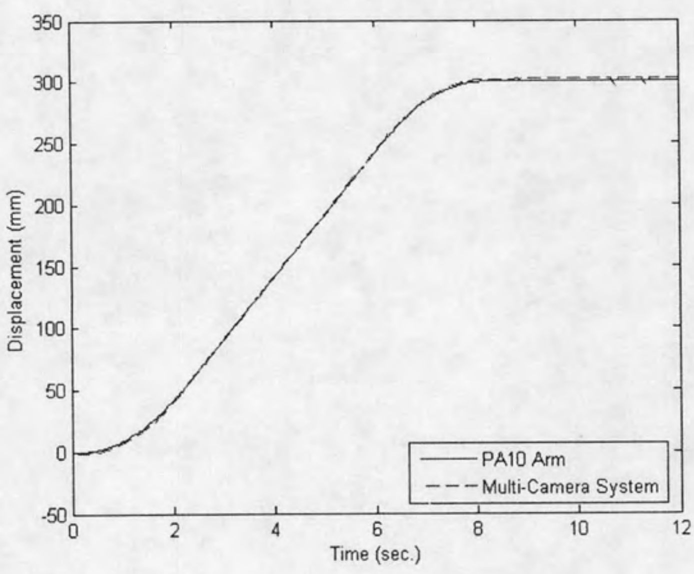

Figure 6.12: Linear motion in x direction of PA10 arm with acceleration and deceleration 25 mm/s^2, velocity 50 mm/s and displacement 300 mm. (3-Cameras)

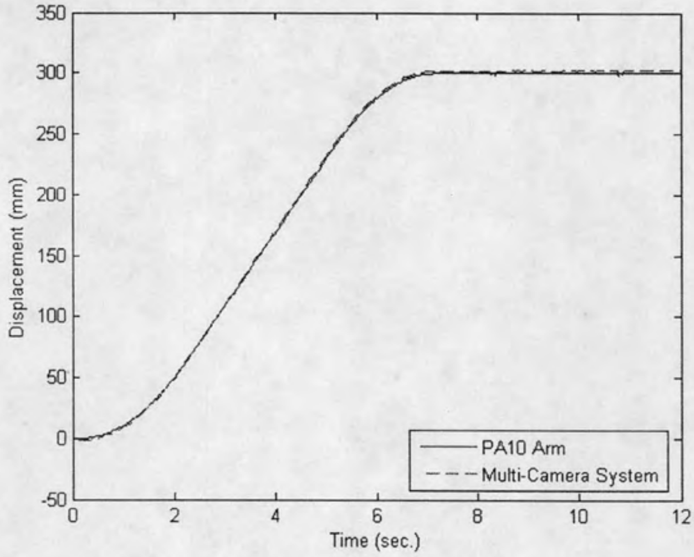

Figure 6.13: Linear motion in x direction of PA10 arm with acceleration and deceleration 30 mm/s^2, velocity 60 mm/s and displacement 300 mm. (3-Cameras)

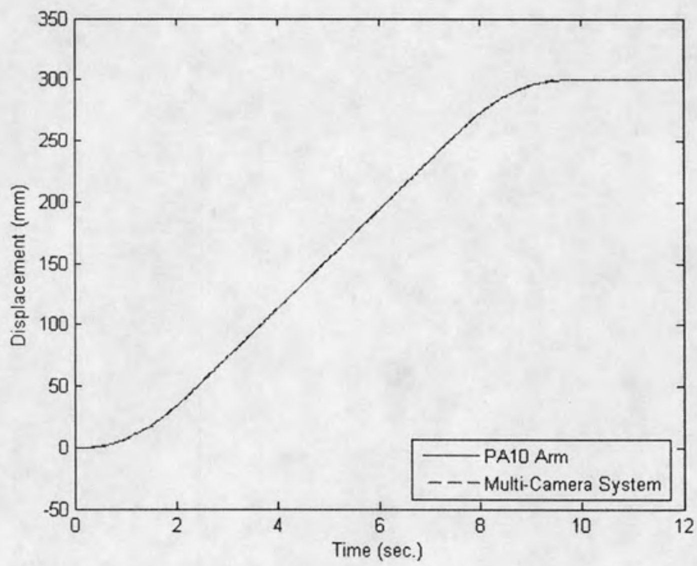

Figure 6.14: Linear motion in y direction of PA10 arm with acceleration and deceleration 20 mm/s^2, velocity 40 mm/s and displacement 300 mm. (3-Cameras)

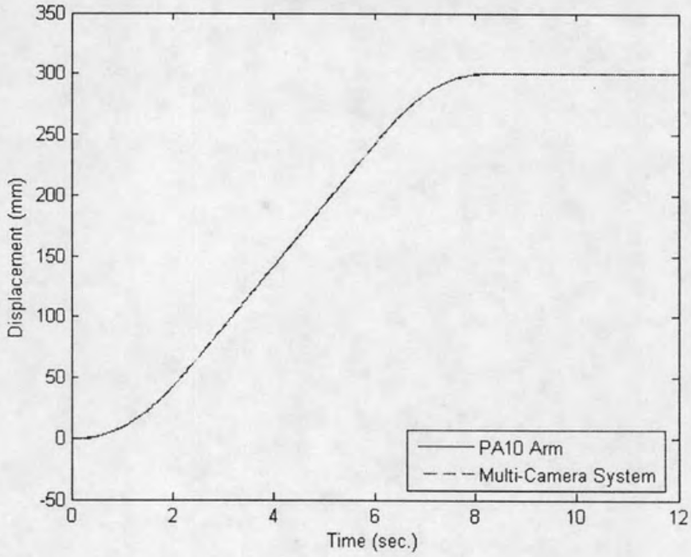

Figure 6.15: Linear motion in y direction of PA10 arm with acceleration and deceleration 25 mm/s^2, velocity 50 mm/s and displacement 300 mm. (3-Cameras)

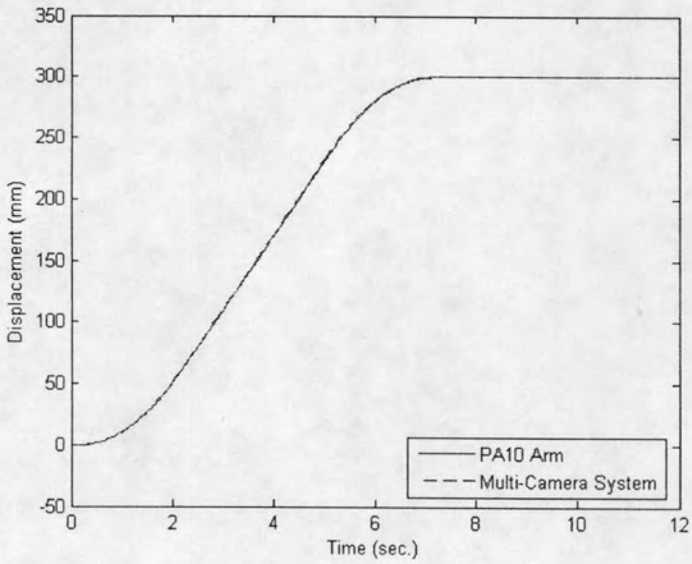

Figure 6.16: Linear motion in y direction of PA10 arm with acceleration and deceleration 30 mm/s^2, velocity 60 mm/s and displacement 300 mm. (3-Cameras)

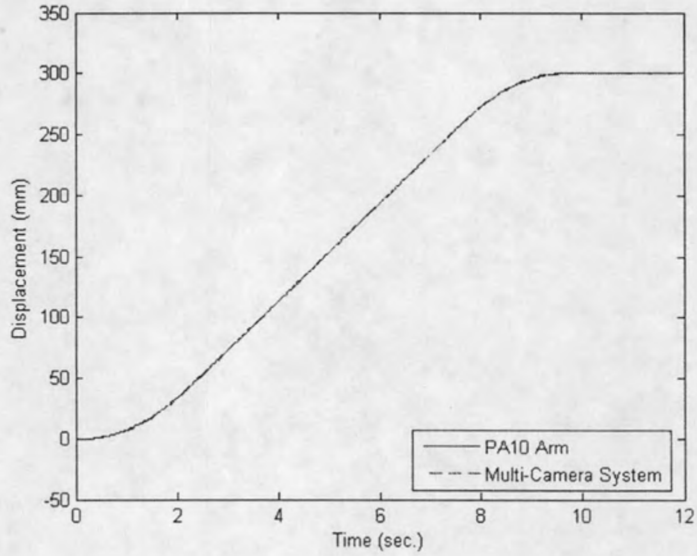

Figure 6.17: Linear motion in z direction of PA10 arm with acceleration and deceleration 20 mm/s^2, velocity 40 mm/s and displacement 300 mm. (3-Cameras)

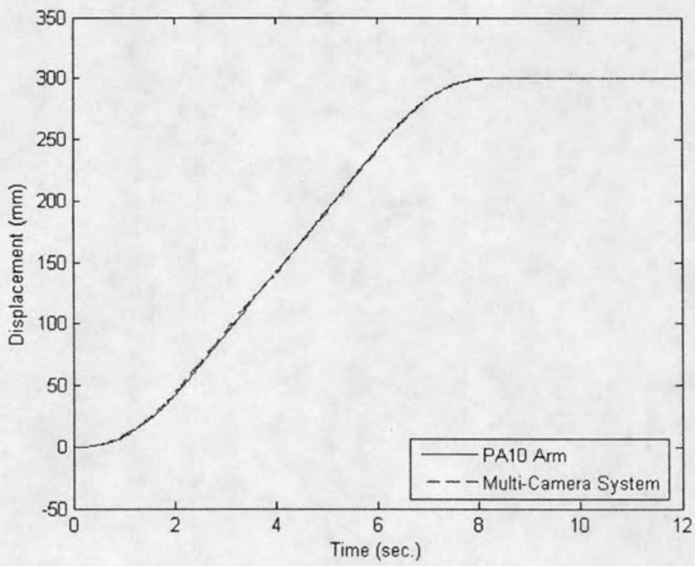

Figure 6.18: Linear motion in z direction of PA10 arm with acceleration and deceleration 25 mm/s^2, velocity 50 mm/s and displacement 300 mm. (3-Cameras)

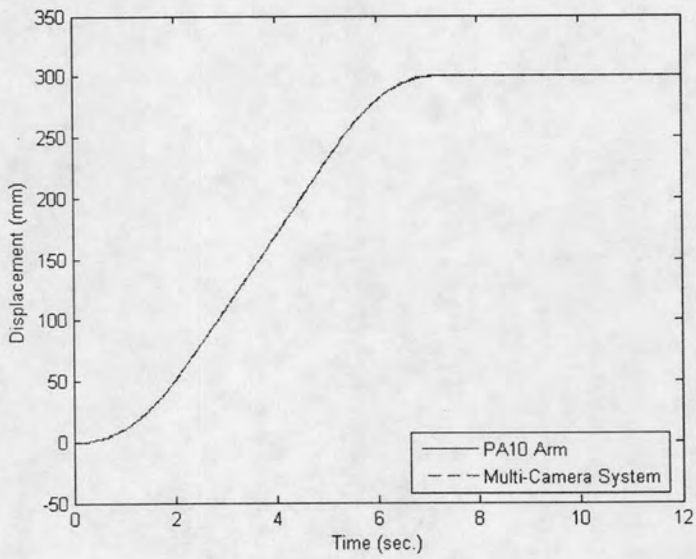

Figure 6.19: Linear motion in z direction of PA10 arm with acceleration and deceleration 30 mm/s^2, velocity 60 mm/s and displacement 300 mm. (3-Cameras)

This experiment shows that the developed system can track moving object, which is a circle with center mark and moves in direct linear path with s-curve velocity profile. The speed of tracking is about 16 fps when use 4 cameras and 18 fps when use 3 cameras. The displacement error at the end of motion when the target moves in x-direction is grater than other directions. However, they are less than 2 mm. in both 3 and 4 cameras.

6.3 3-D Tracking for Circular Motion on a Plane

This experiment was set up for tracking moving object which moves in circular path on planes. PA10-7C arm used to generate paths which are circle with 100 mm in radius. Three planes had been used including xy-plane, yz-plane and zx-plane of PA10-7C. The system had been set up as in section 6.2.

6.3.1 Using 4 Cameras

The following experiment used 4 cameras to track motion of target which is a circle with center mark. The target moved on xy-plane, yz-plane and zx-plane of the PA10-7C arm. The tracking results are shown in figure 6.20–6.25.

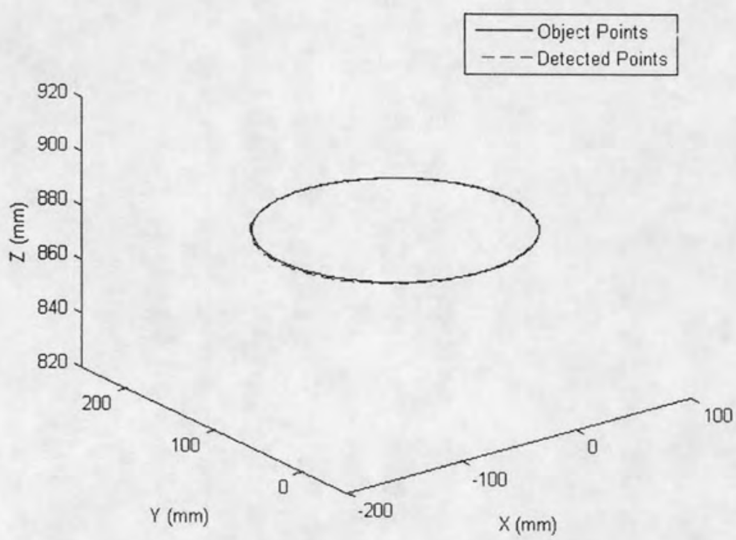

Figure 6.20: Circular motion on xy-plane of PA10-7C arm with angular velocity 0.05 rps. (4-Cameras)

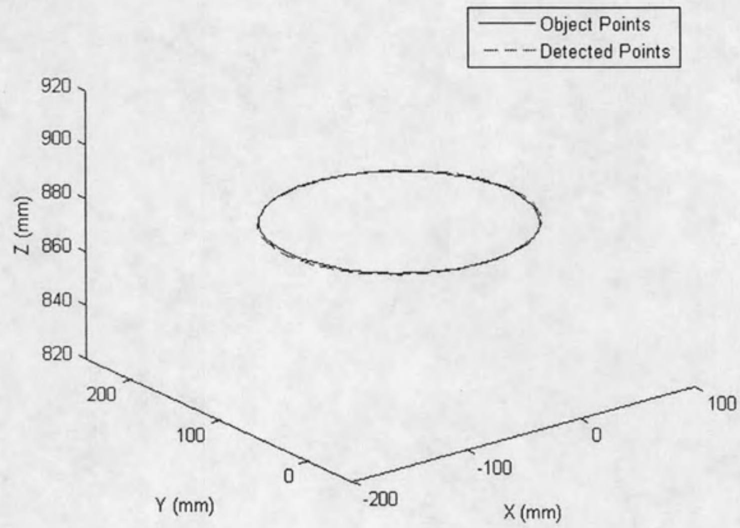

Figure 6.21: Circular motion on xy-plane of PA10-7C arm with angular velocity 0.2 rps. (4-Cameras)

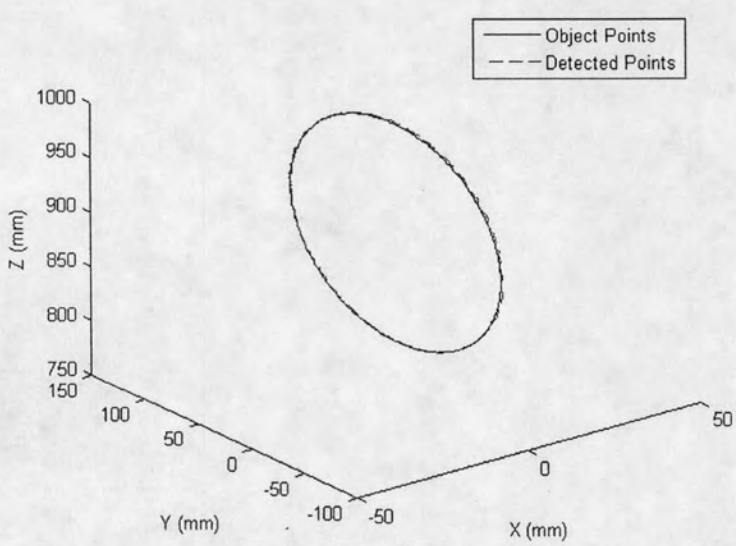

Figure 6.22: Circular motion on yz-plane of PA10-7C arm with angular velocity 0.05 rps. (4-Cameras)

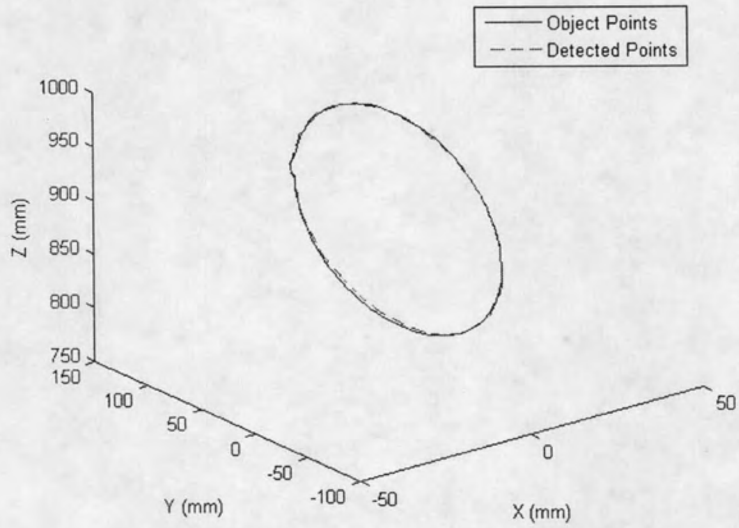

Figure 6.23: Circular motion on yz-plane of PA10-7C arm with angular velocity 0.2 rps. (4-Cameras)

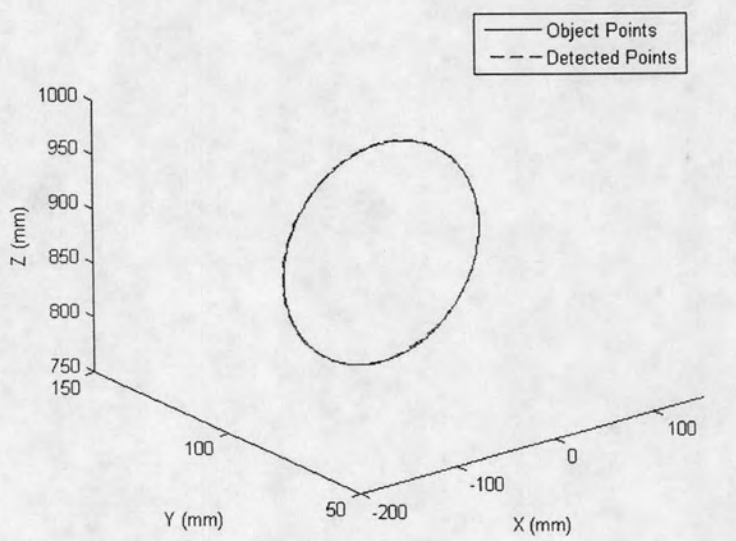

Figure 6.24: Circular motion on zx-plane of PA10-7C arm with angular velocity 0.05 rps. (4-Cameras)

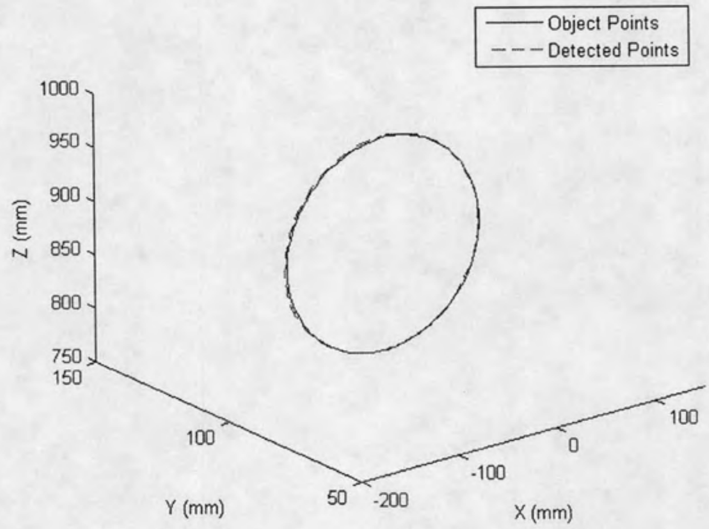

Figure 6.25: Circular motion on zx-plane of PA10-7C arm with angular velocity 0.2 rps. (4-Cameras)

6.3.2 Using 3 Cameras

The following experiment use 3 cameras (without No.1). The tracking results are shown in figure 6.26–6.31.

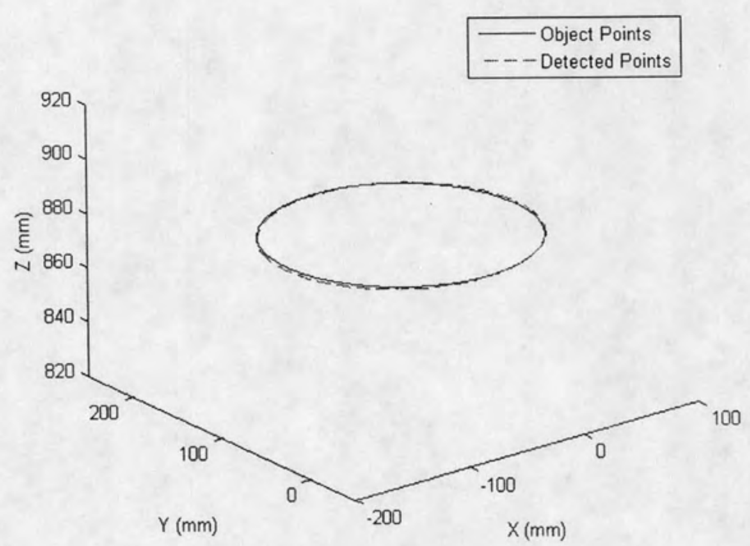

Figure 6.26: Circular motion on xy-plane of PA10-7C arm with angular velocity 0.05 rps. (3-Cameras)

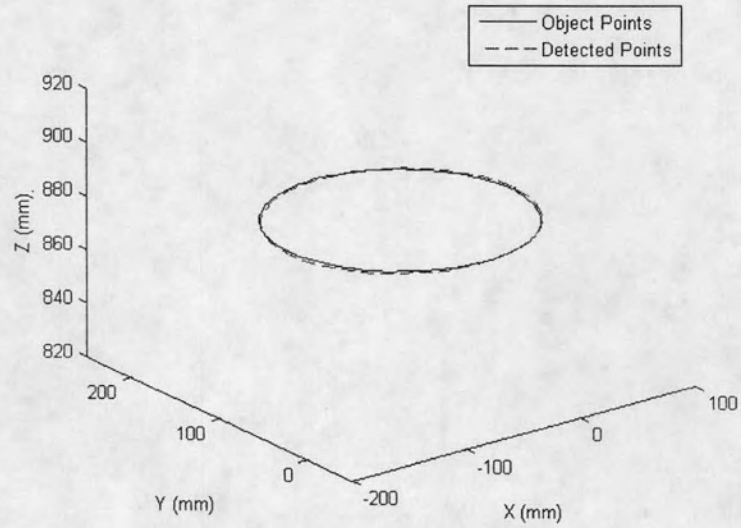

Figure 6. 27: Circular motion on xy-plane of PA10-7C arm with angular velocity 0.2 rps.

(3-Cameras)

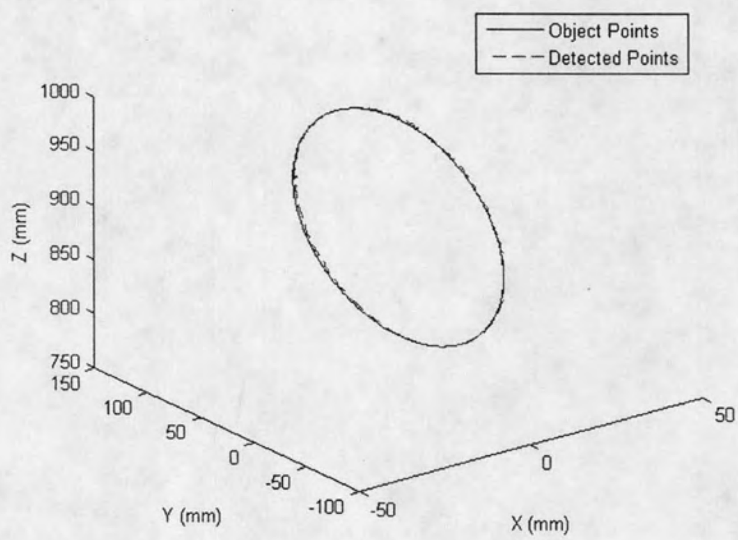

Figure 6.28: Circular motion on yz-plane of PA10-7C arm with angular velocity 0.05 rps.

(3-Cameras)

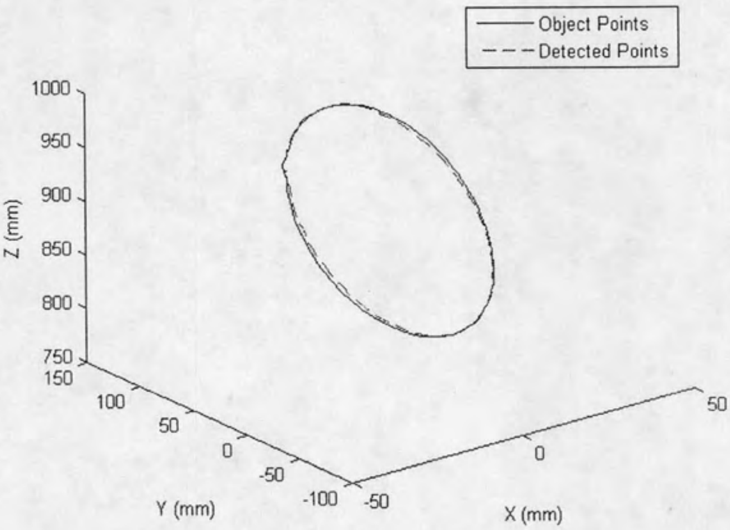

Figure 6.29: Circular motion on yz-plane of PA10-7C arm with angular velocity 0.2 rps. (3-Cameras)

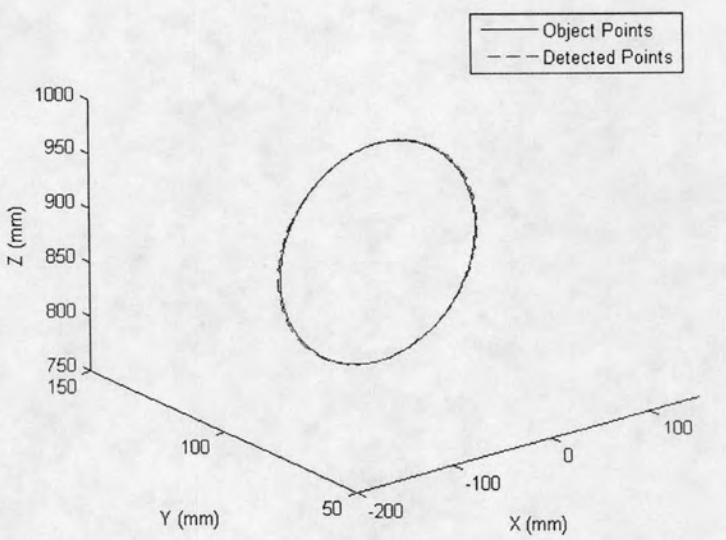

Figure 6.30: Circular motion on zx-plane of PA10-7C arm with angular velocity 0.05 rps. (3-Cameras)

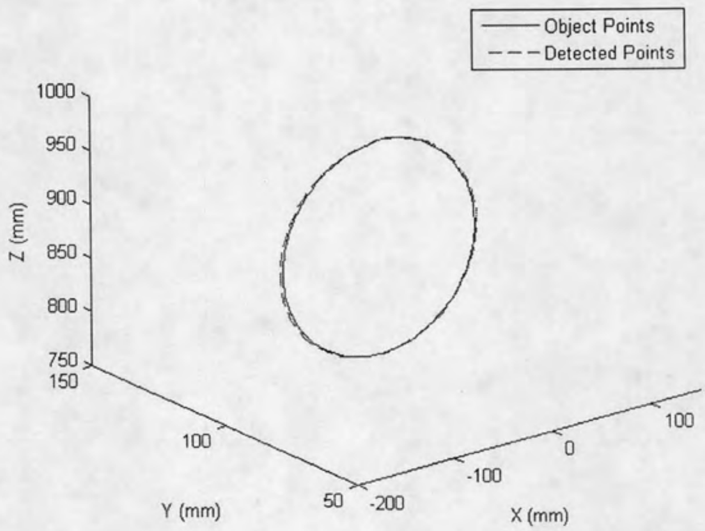

Figure 6.31: Circular motion on zx-plane of PA10-7C arm with angular velocity 0.2 rps. (3-Cameras)

This experiment shows that the developed system can track moving object, which moves in circular path on plane. The speed of tracking is about 16 fps when use 4 cameras and 18 fps when use 3 cameras. From results, the position errors increase when the object moves away from the calibration plane in normal direction (x-direction of PA10-7C arm). For 4-cameras system the errors are less than 1 mm. For 3-cameras system the errors are less than 2 mm except when the object moves on yz-plane of PA10-7C with angular velocity 0.2 rps, the error is slightly greater than 2 mm.

6.4 3-D Tracking for Helical Motion

These experiments were set up for tracking moving object which moves in helical path. PA10-7C arm used to generate paths which are helical with 100 mm in radius and 200 mm in axial displacement. Three helical directions had been used including x, y and z direction of PA10-7C. The system had been set up as in section 6.2.

6.4.1 Using 4 Cameras

The following experiment use 4 cameras to track motion of target which is a circle with center mark. The target moves helically in x-direction, y-direction and z-direction of the PA10-7C arm. The tracking results are shown in figure 6.32–6.37.

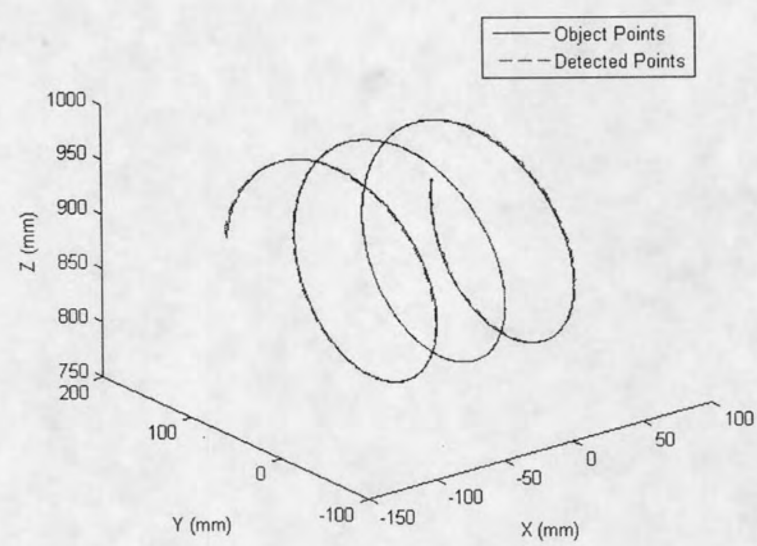

Figure 6.32: Helical motion in x direction with velocity 2.5 mm/s and angular velocity 0.05 rps. (4-Cameras)

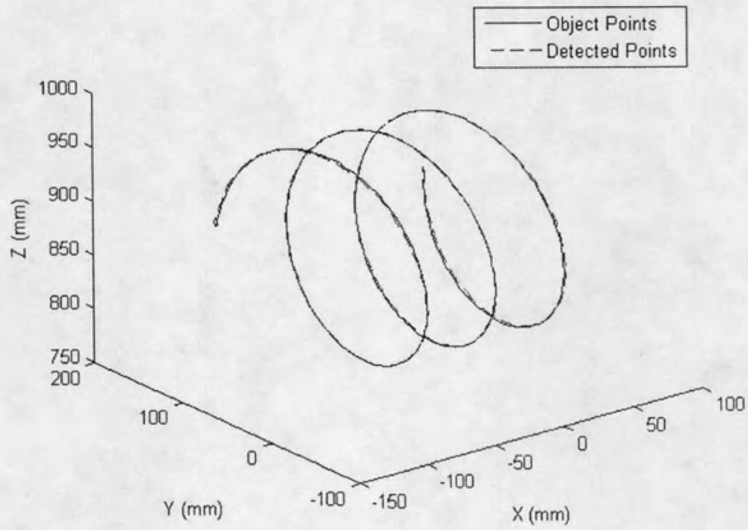

Figure 6.33: Helical motion in x direction with velocity 10 mm/s and angular velocity 0.2 rps. (4-Cameras)

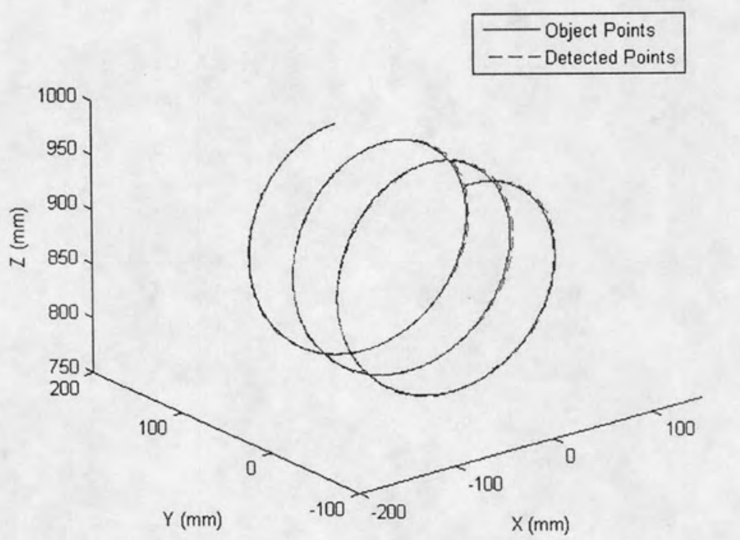

Figure 6.34: Helical motion in y direction with velocity 2.5 mm/s and angular velocity 0.05 rps. (4-Cameras)

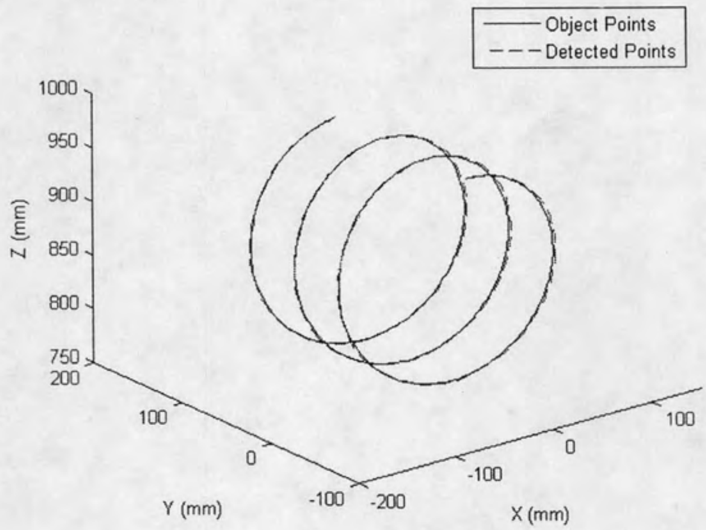

Figure 6.35: Helical motion in y direction with velocity 10 mm/s and angular velocity 0.2 rps. (4-Cameras)

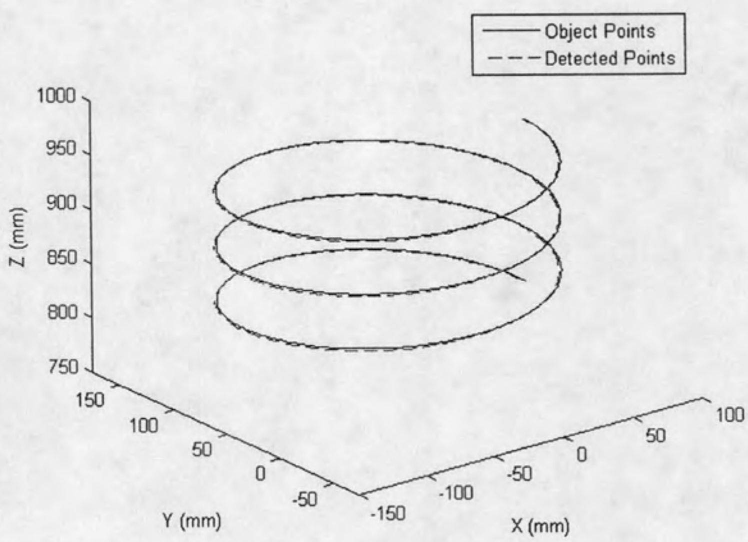

Figure 6.36: Helical motion in z direction with velocity 2.5 mm/s and angular velocity 0.05 rps. (4-Cameras)

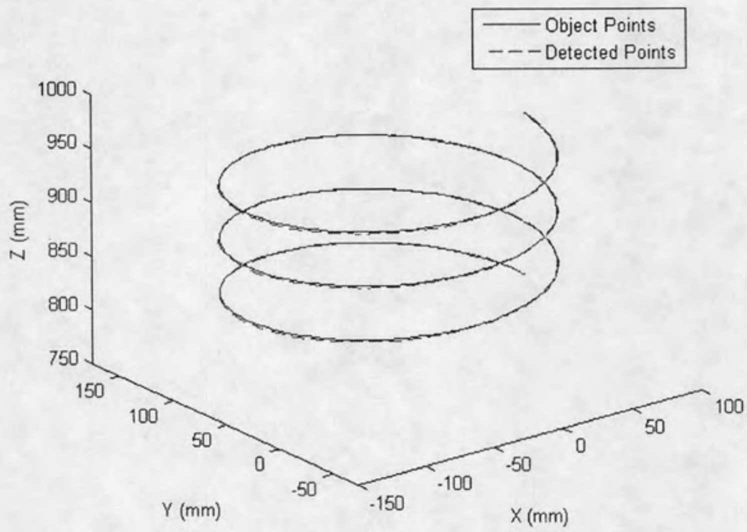

Figure 6.37: Helical motion in z direction with velocity 10 mm/s and angular velocity 0.2 rps. (4-Cameras)

6.4.2 Using 3 Cameras

The following experiment use 3 cameras (without No.1). The tracking results are shown in figure 6.38–6.43.

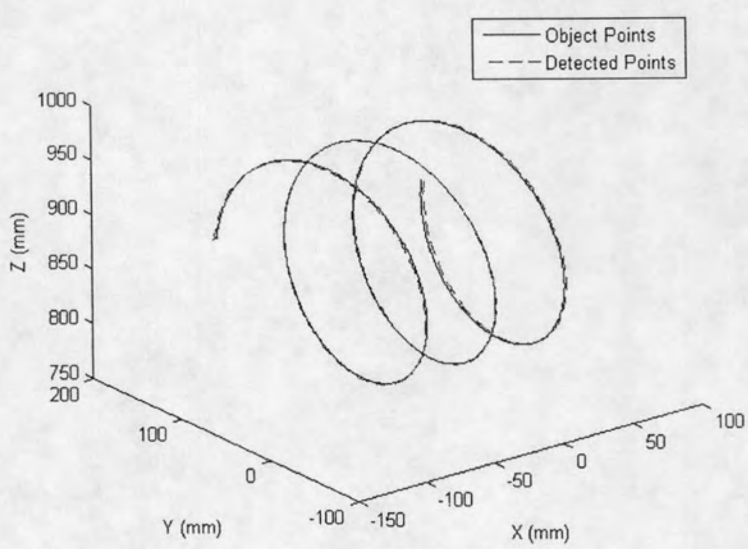

Figure 6.38: Helical motion in x direction with velocity 2.5 mm/s and angular velocity 0.05 rps. (3-Cameras)

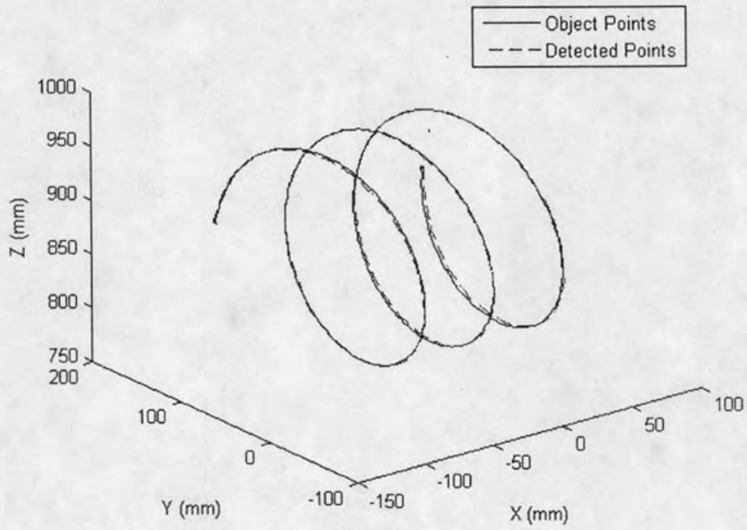

Figure 6.39: Helical motion in x direction with velocity 10 mm/s and angular velocity 0.2 rps. (3-Cameras)

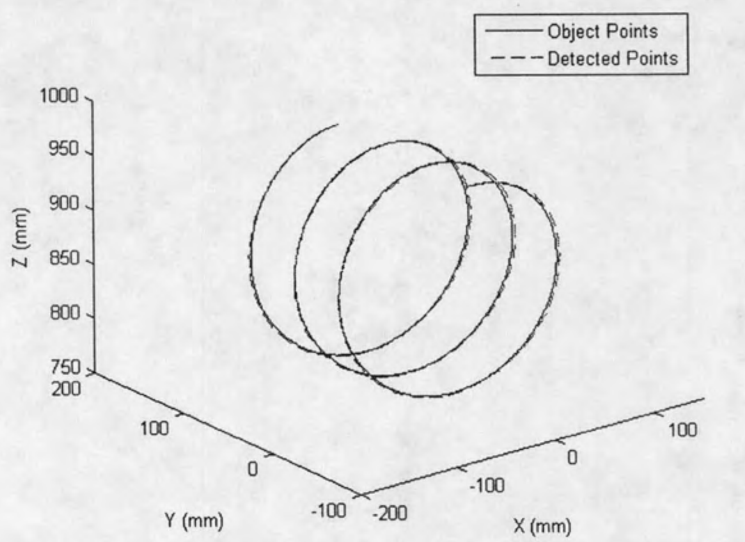

Figure 6.40: Helical motion in y direction with velocity 2.5 mm/s and angular velocity 0.05 rps. (3-Cameras)

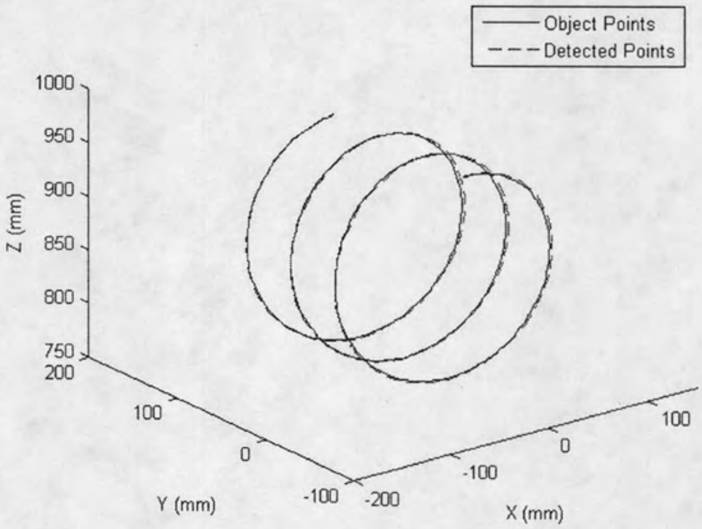

Figure 6.41: Helical motion in y direction with velocity 10 mm/s and angular velocity 0.2 rps. (3-Cameras)

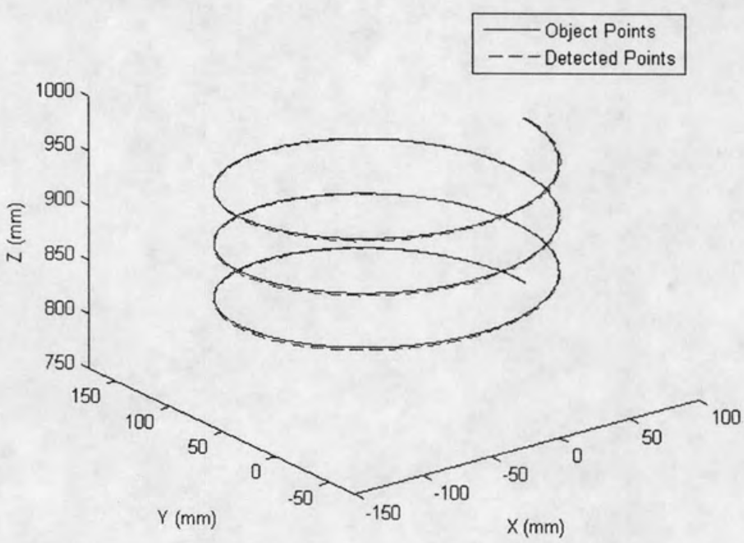

Figure 6.42: Helical motion in z direction with velocity 2.5 mm/s and angular velocity 0.05 rps. (3-Cameras)

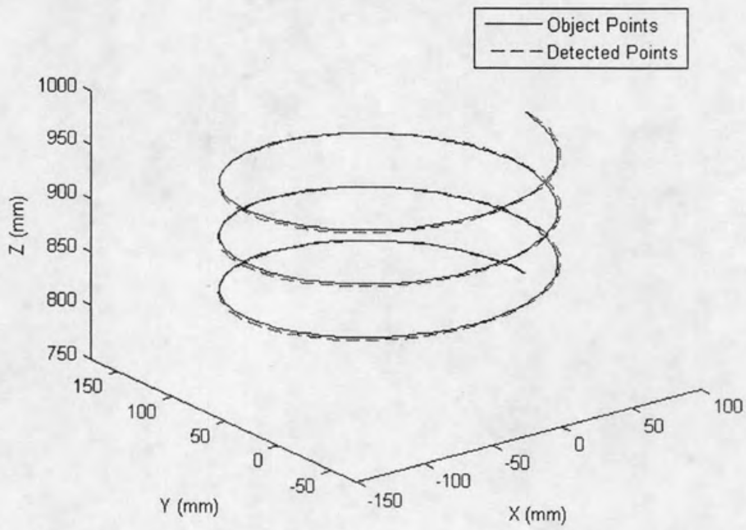

Figure 6.43: Helical motion in z direction with velocity 10 mm/s and angular velocity 0.2 rps. (3-Cameras)

This experiment shows that the developed system can track moving object, which moves in helical path. The speed of tracking is about 16 fps when use 4 cameras and 18 fps when use 3 cameras. From results, the position errors also increase when the object moves away from the calibration plane in normal direction (x-direction of PA10-7C arm). For 4-cameras system the errors are less than 1 mm. For 3-cameras system the errors are less than 2 mm.

6.5 3-D Tracking for 3-D Surface Scanning

This experiment was set up to apply the developed system to measure 3-D surface. The developed system will track 3-D coordinate of the spherical ball, which moved on a 3-D surface. The detected cloud points are offset from original surface with radius of spherical ball. The developed system had been set up as show in figure 6.44 and the camera parameters of camera models are shown in table 6.9. Figure 6.45 shows the original surface which had been used in this experiment. Figure 6.46 shows the detected cloud points and figure 6.47 shows triangular mesh of them.

Table 6.9: Camera parameters of camera models used in 3-D surface scanning.

Parameter	Camera No.1	Camera No.2	Camera No.3	Camera No.4
α_x	2626.3417	2538.6106	2324.1017	2507.2196
α_y	2626.3417	2538.6106	2324.1017	2507.2196
s	0.0000	0.0000	0.0000	0.0000
u_0	640.0000	640.0000	640.0000	640.0000
v_0	480.0000	480.0000	480.0000	480.0000
k_1	0.1758	0.0671	0.0297	-0.1163
k_2	0.0000	0.0000	0.0000	0.0000
R_x	2.2124	2.4879	2.1096	2.6160
R_y	1.4622	0.6433	-1.5765	-0.3226
R_z	-0.4576	-0.2429	0.3607	0.2720
t_x	-0.0807	-0.0842	0.0397	-0.0487
t_y	-0.0351	0.0190	0.0555	0.0550
t_z	0.9727	0.9372	0.8200	0.8420

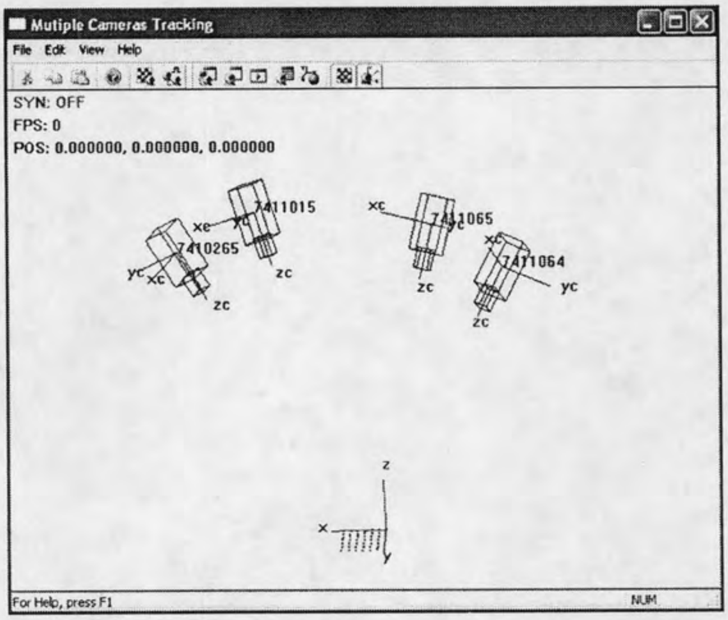

Figure 6.44: Camera models used in 3-D surface scanning experiment.

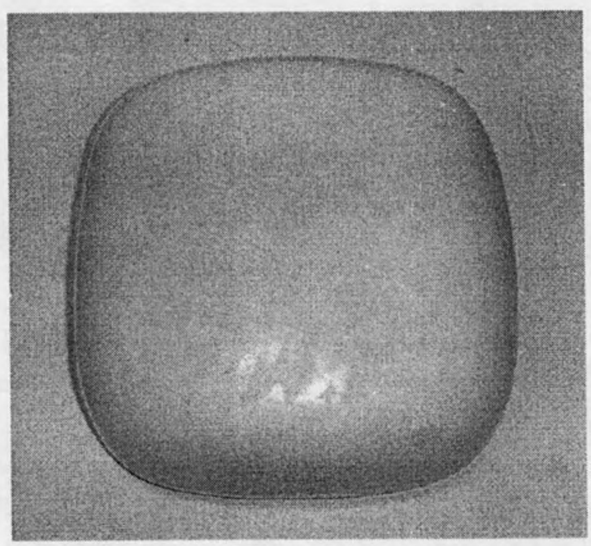

Figure 6.45: Original surface

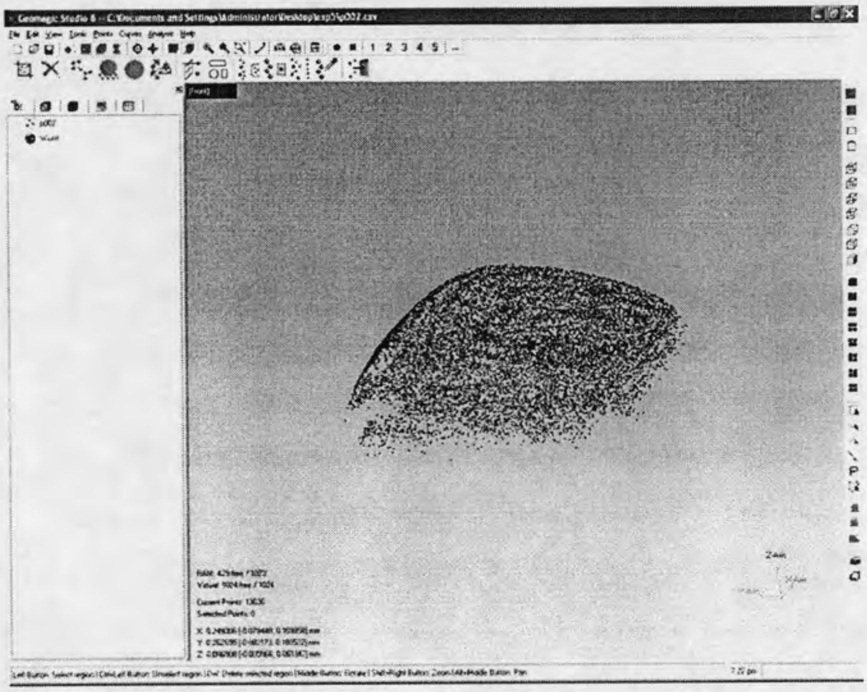

Figure 6.46: Detected cloud points

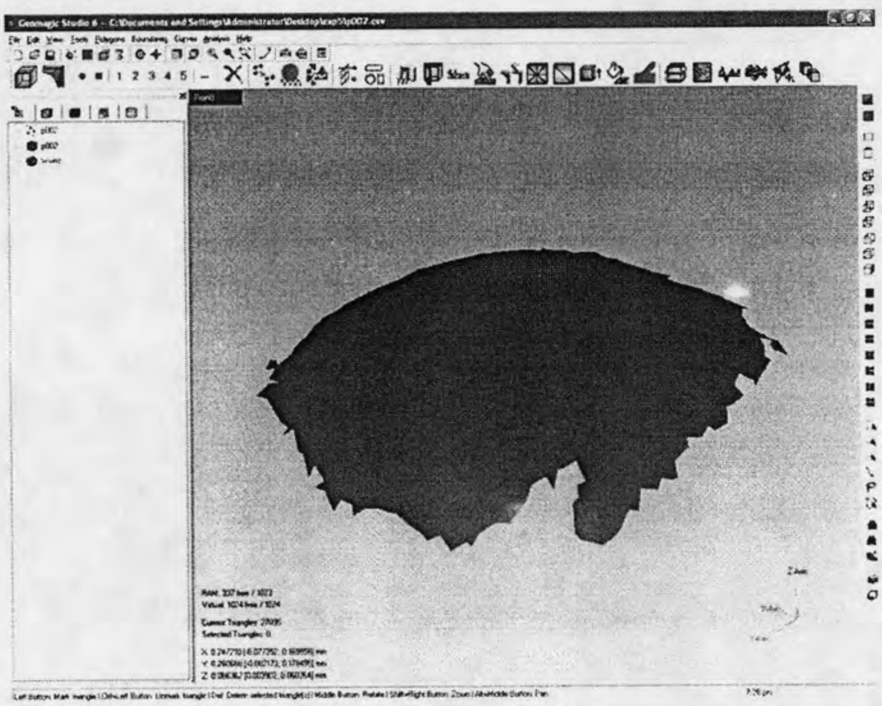

Figure 6.47: Triangular mesh of detected cloud points.